PHYSICAL REVIEW D **90,** 085022 (2014)

Large gauged Q-balls with regular potential

Takashi Tamaki[*]

Department of Physics, General Education, College of Engineering, Nihon University, Tokusada, Tamura, Koriyama, Fukushima 963-8642, Japan

Nobuyuki Sakai[†]

Faculty of Science, Yamaguchi University, Yamaguchi 753-8512, Japan

(Received 6 January 2014; published 23 October 2014)

In many models of gauged Q-balls, which were studied in the literature, there are upper limits for charge Q (and size) of Q-balls due to repulsive Coulomb force. The only known model that allows large Q without limitation is the V-shaped potential, $V \propto |\phi|$, which is singular at $\phi = 0$. To make it clear whether the property of unlimited Q is peculiar to the singular potential, we derive general conditions for potentials that allow Q-balls with unbounded Q. We find that large gauged Q-balls exist even for regular potentials. One of the simple models is $V = (\mu^2/2)\phi^2[1 + K\ln(\phi/M)^2]$ with $K < 0$. We investigate equilibrium solutions for this model systematically. As the electric charge Q increases, the field configuration of the scalar field becomes shell-like; because the charge is concentrated on the surface, the Coulomb force does not destroy the Q-ball configuration. These properties are analogous to those in the V-shaped model. We also find that for each K there is another sequence of unstable solutions, which is separated from the other sequence of the stable solutions. As $|K|$ increases, the two sequences approach; eventually at some point in $-1.07 < K < -1.06$, the "recombination" of the two sequences takes place.

DOI: 10.1103/PhysRevD.90.085022 PACS numbers: 03.75.Lm, 11.27.+d

I. INTRODUCTION

Among nontopological solitons, Q-balls [1] have attracted much attention because they can exist in all supersymmetric extensions of the Standard Model [2]. Specifically, they can be produced efficiently in the Affleck–Dine mechanism [3] and could be responsible for baryon asymmetry [4] and dark matter [5]. Q-balls can also influence the fate of neutron stars [6]. Based on these motivations, stability of Q-balls has been intensively studied [7–9]. These studies have also been extended to general relativistic analysis [10,11] and to different-shaped solitons [12,13].

Another natural extension is introducing U(1) gauge coupling into a scalar field. If we consider an SO(2) symmetric scalar field $\phi = (\phi_1, \phi_2)$, coupling to a gauged field A_μ can be written as

$$\mathcal{S} = \int d^4x \left[\frac{1}{4}F_{\mu\nu}F^{\mu\nu} - \frac{1}{2}\eta^{\mu\nu}D_\mu\phi_a D_\nu\phi_a - V(\phi)\right], \quad (1)$$

where

$$\phi := \sqrt{\phi_a\phi_a}, \qquad F_{\mu\nu} := \partial_\mu A_\nu - \partial_\nu A_\mu, \quad (2)$$

$$D_\mu\phi_a := \partial_\mu\phi_a + A_\mu\epsilon_{ab}\phi_b (a, b = 1, 2). \quad (3)$$

Because such a field is equivalent to electromagnetic field, the conserved charge Q becomes electric charge, and therefore the Coulomb repulsion is expected to disturb formation of large Q-balls. In fact, Lee *et al.* [14] began to study gauged Q-balls with the potential,

$$V_4(\phi) := \frac{m^2}{2}\phi^2 - \lambda\phi^4 + \frac{\phi^6}{M^2} \quad \text{with} \quad m^2, \quad \lambda, \quad M^2 > 0, \quad (4)$$

and claimed that there is a maximum charge and size. To construct large Q-balls, Anagnostopoulos *et al.* [15] introduced fermions with charge of the opposite sign. Li *et al.* [16] assumed a different potential, a piecewise parabolic function, and Deshaies–Jacques and MacKenzie [17] supposed the Maxwell–Chern–Simons theory with the V_4 potential (4) in the $2+1$-dimensional spacetime; it was shown that there is a maximum charge and size of Q-balls in both models.

Arodź and Lis [18] considered gauged Q-balls with the V-shaped potential,

$$V_{\mathrm{V}}(\phi) := \lambda\frac{|\phi|}{\sqrt{2}} \quad \text{with} \quad \lambda > 0. \quad (5)$$

Because its three-dimensional plot has the form of a cone, it would be more appropriate to call it the cone-shaped potential. In addition to normal Q-balls, which have a maximum charge, they found a new type of solutions, Q-shells. Q-shell solutions are obtained in such a way that

[*]tamaki@ge.ce.nihon-u.ac.jp
[†]nsakai@yamaguchi-u.ac.jp

the scalar field and the gauge field are assumed to be constant within a certain sphere $r < r_0$ and the field equations are solved numerically for $r > r_0$. Because the electric charge is concentrated on the shell, large Q-balls with any amount of charge can exist without additional fermions. Thus, this model overcomes the difficulty of the V_4 model. However, the V-shaped potential has another drawback that it is singular at $\phi = 0$.

In this paper, we address the question of whether such large gauged Q-balls can be formed without additional fermions or a singular potential. Gulamov *et al.* [19] pointed out that estimation of the maximum charge in Ref. [14] was incorrect, although they cannot answer the above question since they consider the case in which the gauge field is small. Here, we consider general conditions for regular potentials that allow Q-balls with unbounded charge and investigate equilibrium solutions systematically for one of the models.

This paper is organized as follows. In Sec. II, we show the basic equations of gauged Q-balls. In Sec. III, we discuss general properties of ordinary and gauged Q-balls in the words of Newtonian mechanics. In Sec. IV, we review previous results of V_4 and $V_{\rm V}$ models. In Sec. V, we discuss the general conditions that regular potentials allow Q-balls with unlimited Q. In Sec. VI, we investigate equilibrium solutions systematically for one of the models. Section VII is devoted to concluding remarks.

II. BASIC EQUATIONS

Let us consider the action (1). To find spherically symmetric and equilibrium solutions with vanishing magnetic fields, we assume

$$\phi = \phi(r)(\cos\omega t, \sin\omega t), \quad A_0 = A_0(r), \quad A_i = 0, \tag{6}$$

where the subscript i denotes spatial components and runs 1 to 3. Introducing a variable,

$$\Omega(r) \coloneqq \omega + qA_0(r), \tag{7}$$

we obtain field equations,

$$\frac{d^2\phi}{dr^2} + \frac{2}{r}\frac{d\phi}{dr} + \Omega^2\phi = \frac{dV}{d\phi}, \tag{8}$$

$$\frac{d^2\Omega}{dr^2} + \frac{2}{r}\frac{d\Omega}{dr} = \Omega(q\phi)^2. \tag{9}$$

The boundary condition we assume is

$$\frac{d\phi}{dr}(r=0) = 0, \qquad \frac{d\Omega}{dr}(r=0) = 0, \tag{10}$$

$$\phi(r\to\infty) = 0, \qquad \Omega(r\to\infty) = \omega + \frac{C}{r}, \tag{11}$$

where C is a constant. In numerical calculation, we must choose Ω and ϕ at $\tilde{r} = 0$ to satisfy the asymptotic conditions (11). Concretely, we seek for the appropriate $\phi(0)$ for a fixed $\Omega(0)$.

We define the energy and the charge, respectively, as

$$\begin{aligned} E &= \int d^3x T_{00} \\ &= 2\pi\int_0^\infty r^2 dr\left\{\Omega^2\phi^2 + \left(\frac{d\phi}{dr}\right)^2 + \left(\frac{d\Omega}{dr}\right)^2 + 2V\right\}, \\ Q &= \int d^3x(\phi_1 D_0\phi_2 - \phi_2 D_0\phi_1) \\ &= 4\pi\int_0^\infty r^2\Omega\phi^2 dr, \end{aligned} \tag{12}$$

where T_{00} is the time-time component of the energy-momentum tensor, which is defined by

$$\begin{aligned} T_{\mu\nu} = D_\mu\phi_a D_\nu\phi_a - \eta_{\mu\nu}\left[\frac{1}{2}(D_\lambda\phi_a)^2 + V\right] \\ + F_{\mu\lambda}F^\lambda_\nu - \frac{1}{4}\eta_{\mu\nu}(F_{\lambda\sigma})^2. \end{aligned} \tag{13}$$

Equations (8), (9), and (12) indicate that the sign transformation $\Omega \to -\Omega$ changes nothing but $Q \to -Q$ with keeping E and $\phi(r)$ unchanged. Thus, we choose $\Omega > 0$ in this paper.

III. GENERAL PROPERTIES OF ORDINARY AND GAUGED Q-BALL SOLUTIONS

To begin with, to understand the effect of gauge fields on Q-balls, we review properties of ordinary Q-ball solutions. The field equations are obtained by putting $\Omega = \omega =$ constant in Eq. (8),

$$\frac{d^2\phi}{dr^2} + \frac{2}{r}\frac{d\phi}{dr} = \frac{dV_\omega}{d\phi}, \qquad V_\omega \coloneqq V - \frac{1}{2}\omega^2\phi^2. \tag{14}$$

If one regards the radius r as time and the scalar amplitude $\phi(r)$ as the position of a particle, one can understand solutions in the words of Newtonian mechanics, as shown in Fig. 1. Equation (14) describes a one-dimensional motion of a particle under the nonconserved force due to the effective potential $-V_\omega(\phi)$ and the time-dependent friction $-(2/r)d\phi/dr$. If one chooses the initial position $\phi(0)$ appropriately, the static particle begins to roll down the potential slope, climbs up, and approaches the origin over infinite time.

From the above picture, one can derive the existing conditions of equilibrium solutions of ordinary Q-balls as follows. The first condition is that the initial altitude of the particle $-V_\omega(\phi(0))$ is larger than the final altitude $-V_\omega(\phi(\infty)) = 0$, which leads to

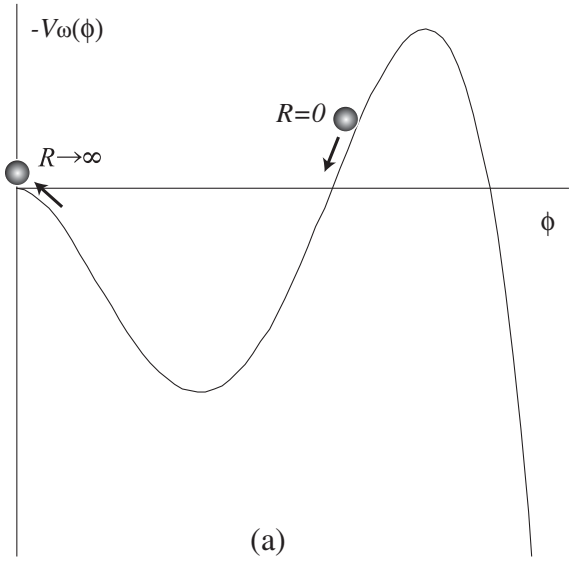

FIG. 1. Interpretation of ordinary Q-balls by analogy with a particle motion in Newtonian mechanics.

$$\max[-V_\omega(\phi)] > 0, \quad \text{i.e.,} \quad \min\left[\frac{2V}{\phi^2}\right] < \omega^2. \tag{15}$$

The second condition is that the particle climbs up at $r \to \infty$, which leads to

$$\lim_{\phi\to+0}\frac{1}{\phi}\left(-\frac{dV_\omega}{d\phi}\right) = \lim_{\phi\to+0}\frac{1}{\phi}\left(\omega^2\phi - \frac{dV}{d\phi}\right) < 0. \tag{16}$$

If the lowest-order term of V is quadratic, i.e., $V = \frac{1}{2}m^2\phi^2 + O(\phi^3)$, the second condition (16) reduces to

$$\omega^2 < m^2 = \frac{d^2V}{d\phi^2}, \tag{17}$$

which gives the upper limit of ω^2. The conditions (15) and (17) were originally obtained by Coleman [1].

However, we cannot apply the second condition (17) to the cone-shape potential $V_{\rm V}$ in (5) because their lowest-order term is not quadratic. Instead, we should go back to the condition (16). In the case of $V_{\rm V}$, if we take $\lambda > 0$, the condition (16) is satisfied regardless of ω. In Sec. V, we discuss general conditions for V that satisfy (16).

Now, let us move on to gauged Q-balls. Without specifying a potential V, we can show that Ω^2 is a monotonically increasing function of r [18]. Using a variable $f := r^2\frac{d\Omega}{dr}$, we can rewrite Eq. (9) as

$$\frac{df}{dr} = \Omega(qr\phi)^2, \qquad \frac{d\Omega}{dr} = \frac{f}{r^2}. \tag{18}$$

The Taylor expansion of Ω and f up to the first order is expressed as

$$f(r+\Delta r) = f(r_0) + (qr_0\phi(r))^2\Omega(r)\Delta r + O(\Delta r^2),$$
$$\Omega(r+\Delta r) = \Omega(r) + \frac{f(r)}{r^2}\Delta r + O(\Delta r^2). \tag{19}$$

By definition, $f(0) = 0$. If $\Omega(0) > 0$, then $f(\Delta r) > 0$. Equation (19) indicates that at every step $r \to r + \Delta r$ both f and Ω increases. Similarly, if $\Omega(0) < 0$, then f and Ω decreases at every step. Thus, we can conclude that Ω^2 is a monotonically increasing function of r.

We can interpret their equilibrium solutions in the words of Newtonian mechanics in the same fashion, except that the potential of a particle is time dependent,

$$V_\Omega = V - \frac{1}{2}\Omega^2\phi^2. \tag{20}$$

Because the potential energy of the particle $-V_\Omega$ increases as the time r increases, the initial altitude $-V_\Omega(0)$ is not necessarily larger than the final altitude $-V_\Omega(\infty) = 0$; that is, there is no condition that corresponds to (15). However, the condition that the particle climbs up at $r \to \infty$ should hold, and we find an existing condition, which corresponds to (16),

$$\lim_{\phi\to+0}\frac{1}{\phi}\left(-\frac{dV_\Omega}{d\phi}\right) = \lim_{\phi\to+0}\frac{1}{\phi}\left(\Omega^2\phi - \frac{dV}{d\phi}\right) < 0. \tag{21}$$

Figure 2 illustrates the time-dependent potential of a fictitious particle $-V_\Omega$. As r increases, Ω^2 also increases; then, $-V_\Omega$ goes up as shown in the figure. There are two types of solutions. One is monotonic solutions as shown in (a): ϕ decreases monotonically as r increases. The other is nonmonotonic solutions as shown in (b): ϕ increases initially, but after the sign of $dV_\Omega/d\phi$ changes, ϕ starts to decrease. The latter type exposes a characteristic of gauged Q-balls, which appears in the $V_{\rm V}$ and other models we shall discuss in Secs. V and VI.

IV. REVIEW OF PREVIOUS RESULTS

In this section, we review gauged Q-ball solutions in the V_4 model [14] and in the $V_{\rm V}$ model [18].

A. V_4 model

For the V_4 model (4), the necessary condition of existing equilibrium solutions (21) is expressed as

$$\lim_{r\to\infty}\Omega^2 < m^2. \tag{22}$$

Because Ω^2 is an increasing function of r, the condition (22) would give a rather strong constraint on the parameter range of existing equilibrium solutions.

We confirm this expectation by numerical calculation as follows. We rescale the quantities as

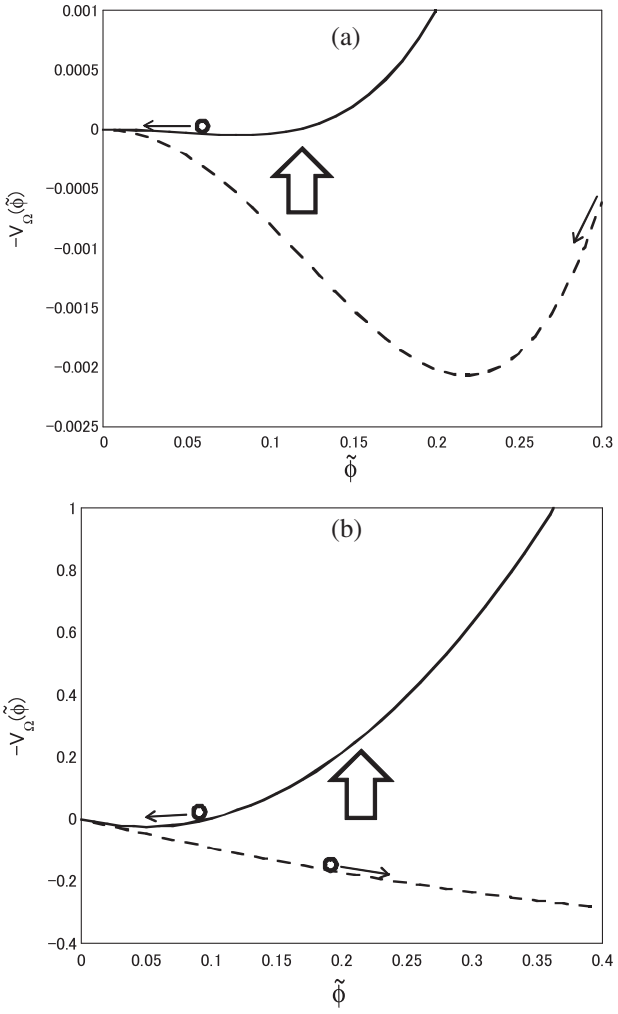

FIG. 2. Interpretation of gauged Q-balls by analogy with a particle motion in Newtonian mechanics. Examples of (a) monotonic solutions in the V_4 model and (b) nonmonotonic solutions in the $V_{\rm V}$ model.

$$\tilde{\phi} \coloneqq \frac{q\phi}{\sqrt{\lambda}M}, \qquad \tilde{\Omega} \coloneqq \frac{\Omega}{\sqrt{\lambda}M},$$
$$\tilde{r} \coloneqq \sqrt{\lambda}Mr, \qquad \tilde{m} \coloneqq \frac{m}{\sqrt{\lambda}M},$$
$$\tilde{Q} \coloneqq q^2Q, \qquad \tilde{E} \coloneqq \frac{q^2E}{\sqrt{\lambda}M}. \tag{23}$$

In Fig. 3, as an example, we show the solution with $\lambda = q = 1$, $\tilde{m}^2 = 0.2$, and $\tilde{Q} = 9$. The dashed and solid lines correspond to the ordinary and gauged Q-balls, respectively. In this solution, the distributions of the scalar field $\tilde{\phi}(\tilde{r})$ almost coincide; however, because $\tilde{\Omega}$ increases as a function of $\tilde{r}$, the condition (22) is narrowly satisfied. Actually, Fig. 2(a) shows the effective potential of this case. Equation (9) tells us that, in order for $\tilde{\Omega}$ to be small in the asymptotic region, $\tilde{r}\tilde{\phi}$ must also be small there; this indicates that $\tilde{Q}$ has an upper limit.

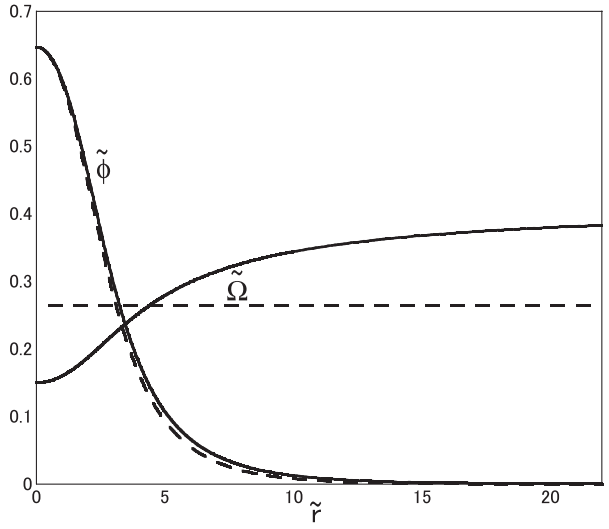

FIG. 3. The field configurations of $\tilde{\phi}$ and $\tilde{\Omega}$ for the V_4 model with $\tilde{m}^2 = 0.2$ and $\tilde{Q} = 9$. The dashed and solid lines correspond to the ordinary and gauged Q-balls, respectively.

B. $V_{\rm V}$ model

Because the $V_{\rm V}$ model (5) has a linear term, the condition (21) is satisfied if $\lambda > 0$. Contrary to the case of the V_4 model, this condition does not put any restriction on Ω. Therefore, large gauged Q-balls are expected in this model.

Using the normalized coupling $\kappa \coloneqq q\lambda/\sqrt{2}$, we rescale the quantities as

$$\tilde{\phi} \coloneqq \frac{q\phi}{\sqrt{\kappa}}, \qquad \tilde{\Omega} \coloneqq \frac{\Omega}{\sqrt{\kappa}}, \qquad \tilde{r} \coloneqq \sqrt{\kappa}r,$$
$$\tilde{Q} \coloneqq q^2Q, \qquad \tilde{E} \coloneqq \frac{q^2E}{\sqrt{\kappa}}. \tag{24}$$

In Fig. 4, we show the field configurations of $\tilde{\phi}$ and $\tilde{\Omega}$ with $\tilde{Q} = 120$. The dashed and solid lines correspond to the ordinary and gauged Q-balls, respectively. In the case of gauged Q-balls, $\tilde{\phi}$ initially increases as a function of $\tilde{r}$ and takes a maximum value at $\tilde{r} = \tilde{r}_{\rm max} \neq 0$; then, it decreases due to the increase of $\tilde{\Omega}$. This behavior can be understood by the effective potential shown in Fig. 2(b). Here, we have defined $\tilde{r}_{\rm max}$ as the value of $\tilde{r}$ where $\tilde{\phi}$ takes a maximum value. In the case of ordinary Q-balls, by contrast, $\tilde{r}_{\rm max}$ is always zero.

We show the $\tilde{\Omega}(0)$-$\tilde{\phi}(0)$ and $\tilde{Q}$-$\tilde{E}$ relations in Figs. 5(a) and 5(b), respectively. The dashed line corresponds to the ordinary Q-balls. The dotted and black solid lines correspond to the gauged case with $\tilde{r}_{\rm max} = 0$ and

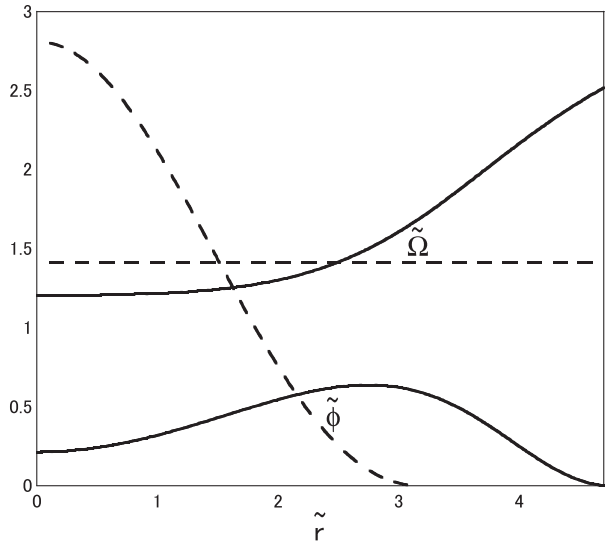

FIG. 4. The field configurations of $\tilde{\phi}$ and $\tilde{\Omega}$ for the $V_{\rm V}$ model with $\tilde{Q} = 120$. The dashed and solid lines correspond to the ordinary and gauged Q-balls, respectively.

that with $\tilde{r}_{\rm max} \neq 0$, respectively. The blue solid line corresponds to the Q-shell solutions that will be explained below.

In the case of ordinary Q-balls ($\tilde{\Omega} = \tilde{\omega}$), the $\tilde{\Omega}(0)$-$\tilde{\phi}(0)$ relation, which was represented by the dashed line in Fig. 5(a), can be understood as follows. In the picture of a particle motion in Newtonian mechanics, if we ignore the "nonconserved force" term, $(2/r)d\phi/dr$, the maximum of $\tilde{\phi}$, $\tilde{\phi}_{\rm max} = \tilde{\phi}(0)$ is determined by the nontrivial solution of $V_\Omega = 0$. Then, we obtain

$$\tilde{\phi}(0) = \frac{2}{\tilde{\Omega}^2}, \tag{25}$$

which approximates the dashed line in (a).

In the case of gauged Q-balls, the $\tilde{\Omega}(0)$-$\tilde{\phi}(0)$ relation for large $\tilde{\Omega}(0)$ (small $\tilde{Q}$), which is represented by the dotted line in Fig. 5(a), almost coincides with that for ordinary Q-balls. For small $\tilde{\Omega}(0)$ (large $\tilde{Q}$), however, the $\tilde{\Omega}(0)$-$\tilde{\phi}(0)$ relation for ordinary Q-balls and that for gauged Q-balls are qualitatively different. Nevertheless, it is surprising that there is no qualitative difference in the $\tilde{Q}$-$\tilde{E}$ relation between solutions with $\tilde{r}_{\rm max} = 0$ and those with $\tilde{r}_{\rm max} \neq 0$. Both solutions are on the same quasilinear relation across point A.

Q reaches a maximum at the point B where cusp structure appears in the $\tilde{Q}$-$\tilde{E}$ plane. Q-ball solutions with the boundary conditions (10) disappear at the point C where $\tilde{\phi}(0) \to 0$. However, Arodź and Lis [18] found a new type of solutions with boundary conditions (11) and

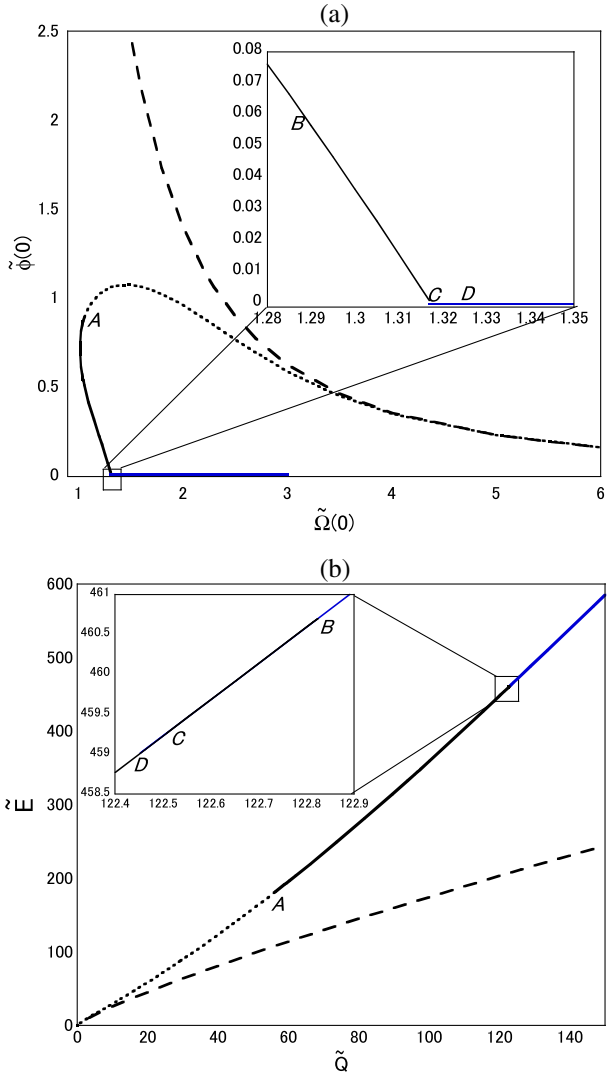

FIG. 5 (color online). (a) $\tilde{\Omega}(0)$-$\tilde{\phi}(0)$ and (b) $\tilde{Q}$-$\tilde{E}$ relations for the $V_{\rm V}$ model. The dashed line corresponds to the ordinary Q-balls. The dotted and black solid lines correspond to the gauged Q-balls with $\tilde{r}_{\rm max} = 0$ and those with $\tilde{r}_{\rm max} \neq 0$, respectively. The blue solid line corresponds to the Q-shell solutions.

$$\phi(r) = \frac{d\phi}{dr}(r) = \frac{d\Omega}{dr}(r) = 0, \quad \text{for } 0 < r < r_0, \tag{26}$$

which are different from (10), and called them "Q-shells." The $\tilde{Q}$-$\tilde{E}$ curve of Q-shells is smoothly connected to that of Q-balls at point C. As $\tilde{\Omega}(0)$ increases, Q decreases and reaches a minimum at another cusp D in the $\tilde{Q}$-$\tilde{E}$ plane; then, Q turns to increase without upper limit. We also show the $\tilde{Q}$-$(\tilde{E} - 3.7459\tilde{Q})$ relation in Fig. 6, where we see that the solutions B-C-D have slightly larger values of $\tilde{E}$ than those of the other solutions with the same Q. If we apply the catastrophe theory [20], we find that the solution sequence B-C-D is unstable, while the other two sequences are stable and cross in the $\tilde{Q}$-$\tilde{E}$ plane.

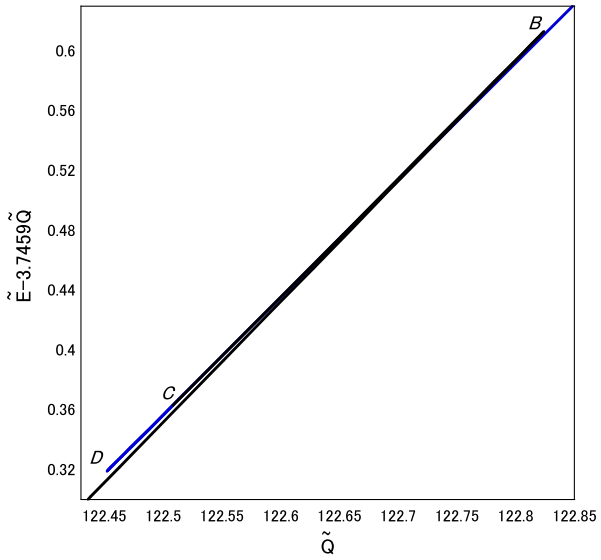

FIG. 6 (color online). $\tilde{Q}$-$(\tilde{E}-3.7459\tilde{Q})$ relation for the V_{V} model near the points B, C, and D.

V. CONDITIONS FOR REGULAR POTENTIALS THAT ALLOW UNBOUNDED CHARGE

Now, we discuss whether any regular potentials allow Q-balls with unlimited Q. As we discussed in the previous section, to obtain large $\tilde{Q}$ solutions, $\tilde{\Omega}$ should become so large without violating the condition (21). $\tilde{\Omega}$ is not constrained by (21) at all if and only if

$$\lim_{\phi\to+0}\frac{1}{\phi}\frac{dV}{d\phi}=\infty. \tag{27}$$

This is the general condition for V that allows large Q-balls without limitation.

We also require the regularity condition at the center,

$$\lim_{\phi_1\to+0}\frac{\partial V}{\partial\phi_1}=\lim_{\phi_1\to-0}\frac{\partial V}{\partial\phi_1}, \tag{28}$$

for $\phi_2=0$. This condition is equivalent to

$$\lim_{\phi\to+0}\frac{dV}{d\phi}=0. \tag{29}$$

Next, we investigate concrete expressions of V that satisfy (27) and (29). We denote the dominant term of V at $\phi\approx 0$ by $V_0(\phi)$ and discuss two types of functions for V_0:

(i) Suppose

$$V_0=K\phi^{\alpha}, \tag{30}$$

where α is a positive real number. Because

$$\frac{1}{\phi}\frac{dV_0}{d\phi}=K\alpha\phi^{\alpha-2}, \tag{31}$$

the condition that (27) is satisfied is given by

$$\alpha<2, \qquad K>0. \tag{32}$$

The V-shaped potential ($\alpha=1$) falls into this class. However, if we take account of the regularity condition (29), which indicates $\alpha>1$, the allowed parameter range of α becomes

$$1<\alpha<2. \tag{33}$$

Note that integers are not allowed for the power α.

(ii) Suppose a more general class,

$$V_0=K\phi^{\alpha}\left(\log\frac{\phi}{M}\right)^n, \tag{34}$$

where α is a positive real number and n is a natural number. Because

$$\begin{aligned}\frac{1}{\phi}\frac{dV_0}{d\phi}&=K\phi^{\alpha-2}\left(\log\frac{\phi}{M}\right)^{n-1}\left(\alpha\log\frac{\phi}{M}+n\right)\\&\approx K\alpha\phi^{\alpha-2}\left(\log\frac{\phi}{M}\right)^n,\end{aligned} \tag{35}$$

the condition (27) is satisfied if

$$\alpha\le 2, \quad \{n\,\text{is odd}, K<0\} \quad \text{or} \quad \{n\,\text{is even}, K>0\}. \tag{36}$$

Because the regularity condition (29) indicates $\alpha>1$, the allowed parameter range of α becomes

$$1<\alpha\le 2. \tag{37}$$

One of the simple choices is $\alpha=2, n=1$, and, accordingly, $K<0$:

$$V_0=K\phi^2\log\left(\frac{\phi}{M}\right). \tag{38}$$

If we include the regular mass term $\mu^2\phi^2/2$ and redefine K, we have

$$V_{\log}=\frac{\mu^2}{2}\phi^2\left[1+K\phi^2\log\left(\frac{\phi}{M}\right)\right]. \tag{39}$$

This agrees with the gravity-mediated type in the Affleck–Dine mechanism. In the next section, we investigate equilibrium solutions for this model systematically.

VI. LOG POTENTIAL

We rescale the quantities in (39) as

$$\tilde{\phi} \coloneqq \frac{q\phi}{M}, \qquad \tilde{\Omega} \coloneqq \frac{\Omega}{M},$$
$$\tilde{r} \coloneqq Mr, \qquad \tilde{\mu} \coloneqq \frac{\mu}{M},$$
$$\tilde{Q} \coloneqq q^2 Q, \qquad \tilde{E} \coloneqq \frac{q^2 E}{M}. \tag{40}$$

We fix $\tilde{\mu} = q = 1$ below.

We show some solutions of gauged Q-balls in Fig. 7; we choose $K = -1$ and obtain solutions with $\tilde{Q} = 1.7$ and 11, in which case $r_{\max} = 0$, and that with $\tilde{Q} = 103$, in which case $r_{\max} \neq 0$. As $\tilde{Q}$ increases, the field configuration becomes shell-like, and the location of the shell becomes farther from the center. This behavior is explained by the repulsive Coulomb force of electric charge. These configurations are just like "Q-shells," which were obtained by Arodź and Lis for the V-shaped model [18]. The difference is that we use the boundary conditions (10) and (11) consistently and give a tiny but nonzero value for $\tilde{\phi}(0)$, while they adopted the special boundary condition (26).

We show the $\tilde{\Omega}(0)$-$\tilde{\phi}(0)$ and $\tilde{Q}$-$\tilde{E}$ relations for $K = -1$ in Fig. 8. For reference, we also plot the relations for ordinary Q-balls ($\Omega = \omega$), which are represented by the dashed lines. Their extreme behavior in the thin-wall limit ($\omega \to \infty$) and in the thick-wall limit ($\omega \to 0$) can be discussed analytically as follows [13]. The maximum of ϕ, $\tilde{\phi}_{\max} = \tilde{\phi}(0)$, can be estimated by the nontrivial solution of $V_\Omega = 0$:

$$\tilde{\phi}_{\max} = e^{\frac{1-\tilde{\omega}^2}{-2K}}. \tag{41}$$

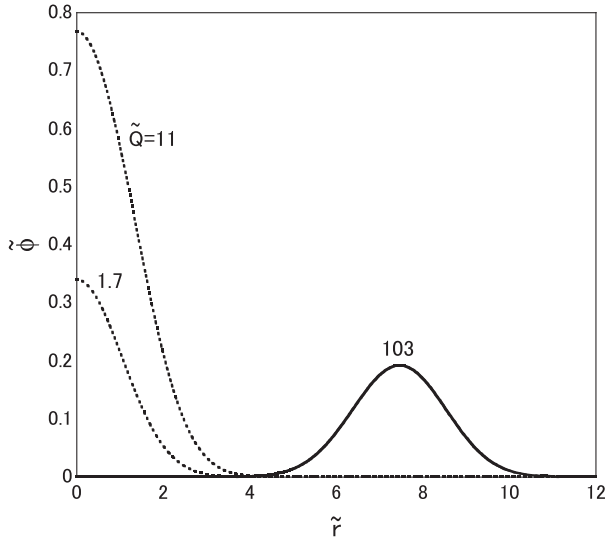

FIG. 7. The field configurations of $\tilde{\phi}$ for gauged Q-balls with $K = -1$ and $\tilde{Q} \simeq 1.7$, 11, and 103.

Because the energy and the charge are roughly estimated as

$$E \sim V(\phi_{\max})R^3, \qquad Q \sim \omega\phi_{\max}^2 R^3, \tag{42}$$

where R is the typical radius, we find

$$\omega \to 0 : \phi_{\max} \to \text{nzf}, \qquad E \to \text{nzf}, \qquad Q \to 0,$$
$$\omega \to \infty : \phi_{\max} \to 0, \qquad E \to 0, \qquad Q \to 0, \tag{43}$$

where nzf denotes nonzero finite. Therefore, there is an upper limit $Q_{\max}$. This analytic estimate agrees with the numerical results in Fig. 8. There are two sequences of solutions that merge at the cusp. We suppose by energetics

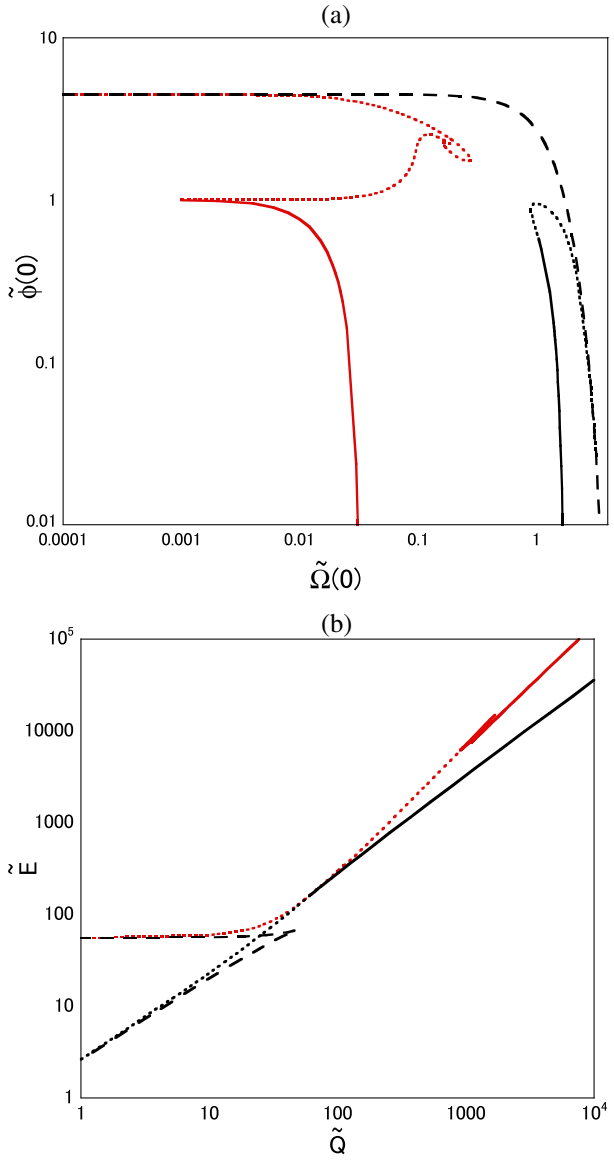

FIG. 8 (color online). (a) $\tilde{\Omega}(0)$-$\tilde{\phi}(0)$ and (b) $\tilde{Q}$-$\tilde{E}$ relations for $K = -1$. The dashed lines correspond to ordinary Q-balls. The dotted and solid lines correspond to gauged Q-balls with $\tilde{r}_{\max} = 0$ and those with $\tilde{r}_{\max} \neq 0$, respectively.

that the sequences with high energy are unstable (unstable branch) while those with low energy are stable (stable branch).

The results for gauge Q-balls are represented by the dashed lines ($\tilde{r}_{\max} = 0$) and the solid lines ($\tilde{r}_{\max} \neq 0$). The solutions denoted by red lines correspond to those with small ω and an unstable branch, while those denoted by black lines correspond to large ω and a stable branch. For dotted lines, the gauged Q-balls are similar to the ordinary Q-balls (dashed lines). In contrast, due to the non-monotonic behavior of $\tilde{\phi}(\tilde{r})$ (i.e., $\tilde{r}_{\max} \neq 0$), the properties of gauged Q-balls with solid lines and ordinary Q-balls are quite different.

As for the stable solutions denoted by the black lines, both $\tilde{\Omega}(0)$-$\tilde{\phi}(0)$ and $\tilde{Q}$-$\tilde{E}$ relations of solutions are similar to those of the $V_{\rm V}$ model, except that the cusp structure does not appear in the $\tilde{Q}$-$\tilde{E}$ plane in Fig. 8(b). Because $\tilde{E}$ is a monotonically increasing function of $\tilde{Q}$, we judge that all equilibrium solutions by black lines are stable. We also suppose by energetics that the solutions denoted by red lines are unstable.

Figures 9 and 10 show the $\tilde{\Omega}(0)$-$\tilde{\phi}(0)$ and $\tilde{Q}$-$\tilde{E}$ relations for $K = -0.6$ and -0.4, respectively. We find that as $|K|$ decreases the existing domain of the unstable solutions becomes small in the $\tilde{\Omega}(0)$-$\tilde{\phi}(0)$ plane, and the two sequences leave away from each other.

A drastic change occurs between $K = -1.06$ and $K = -1.07$, as shown in Figs. 11 and 12. As $|K|$ increases, the two sequences approach further; eventually at some point in $-1.07 < K < -1.06$, the "recombination" of the

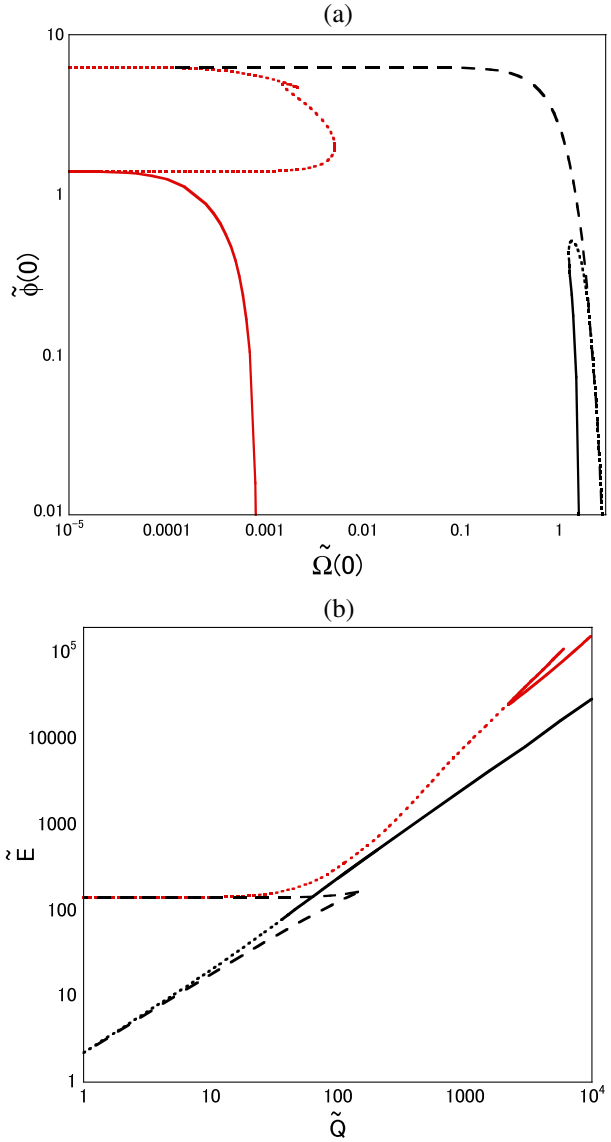

FIG. 9 (color online). (a) $\tilde{\Omega}(0)$-$\tilde{\phi}(0)$ and (b) $\tilde{Q}$-$\tilde{E}$ relations for $K = -0.6$.

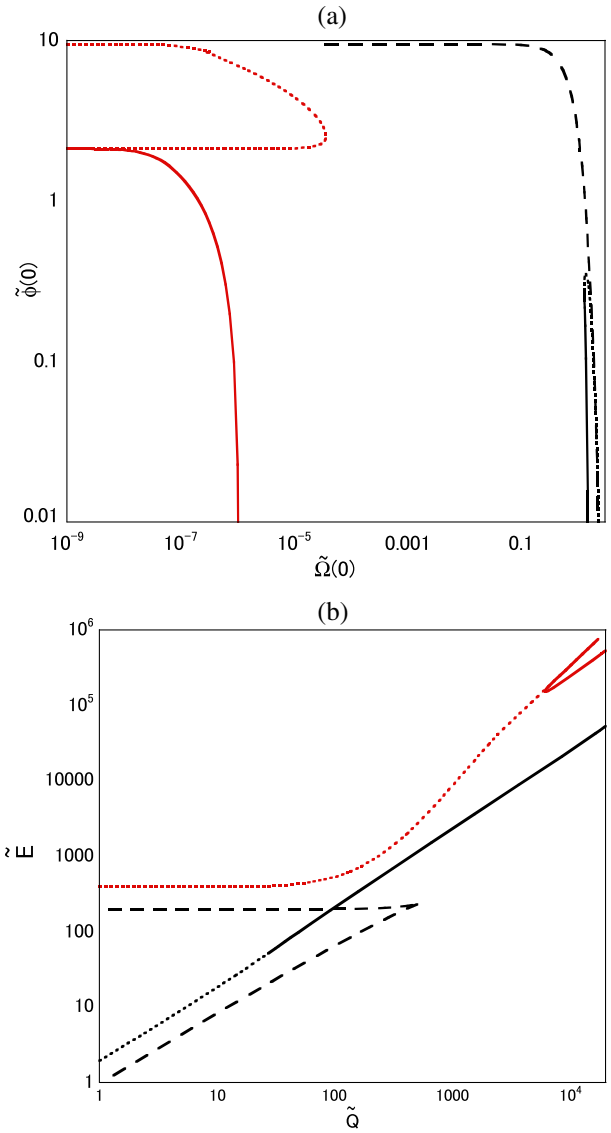

FIG. 10 (color online). (a) $\tilde{\Omega}(0)$-$\tilde{\phi}(0)$ and (b) $\tilde{Q}$-$\tilde{E}$ relations for $K = -0.4$.

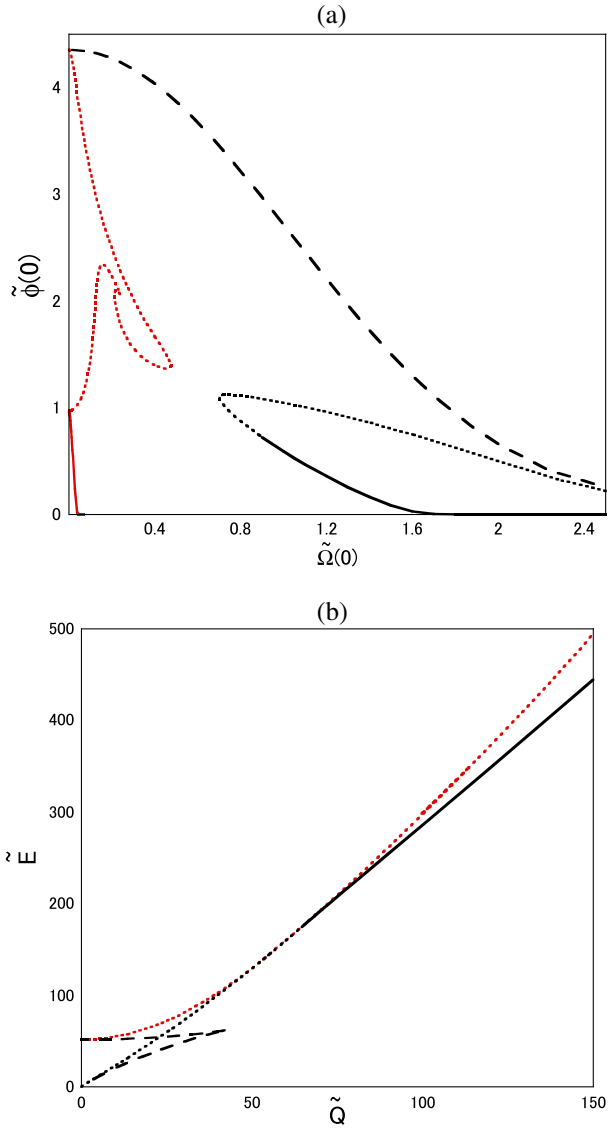

FIG. 11 (color online). (a) $\tilde{\Omega}(0)$-$\tilde{\phi}(0)$ and (b) $\tilde{Q}$-$\tilde{E}$ relations for $K = -1.06$. The two sequences in red lines and in black lines are about to touch.

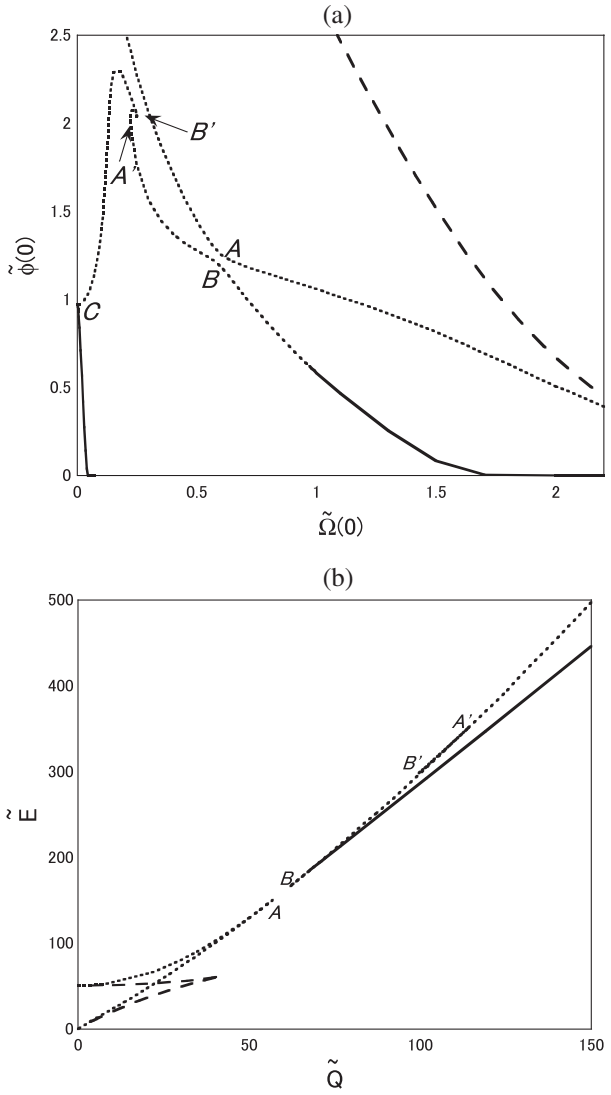

FIG. 12. (a) $\tilde{\Omega}(0)$-$\tilde{\phi}(0)$ and (b) $\tilde{Q}$-$\tilde{E}$ relations with $K = -1.07$. The recombination of the two sequences happens.

two sequences takes place. At first sight, this recombination looks strange; however, we can understand this phenomenon in a rational way as follows. If we look at the existing domain of equilibrium solutions in the two-dimensional parameter space [say, the $\tilde{\Omega}(0)$-$\tilde{\phi}(0)$ or the $\tilde{Q}$-$\tilde{E}$ space] for fixed K, we see that there are two separate sequences of solutions. However, if we consider the existing domain in the three-dimensional parameter by regarding K as another parameter, it is described by a simply connected surface. The recombination of the two sequences is nothing but changing cross sections of the same surface.

The solution sequence of the ordinary Q-balls, represented by the dashed line in Fig. 12, is analogous to the sequence including point A. The other sequence including point B has no counterpart of ordinary Q-balls. The solutions in the branch B-A'-B' are unstable, and there are two small cusps about A'-B'. The lower energy solutions in both sequences are stable; interestingly, the two sequences of stable solutions are separated. There is no upper limit of $\tilde{Q}$.

As a common property for every K, there are sequences of cusp structures in the large Q region for unstable solutions. We show (a) $\tilde{\Omega}(0)$-$\tilde{\phi}(0)$ and (b) $\tilde{Q}$-$\tilde{E}$ relations for the very small $\tilde{\phi}(0)$ (and large $\tilde{Q} > 500$) region for $K = -1.07$ in Fig. 13. Complicated structure appears along the sequence C to G; there are several cusps about C-D-E-F. As shown in Fig. 14, field distributions in this region also have complicated structures. Beyond the point F, both $\tilde{\phi}_{\max}$ and $\tilde{r}_{\max}$ monotonically increase. It is interesting that small differences of boundary values $\tilde{\Omega}(0)$ and $\tilde{\phi}(0)$ result in such large differences in $\tilde{Q}$ and $\tilde{E}$.

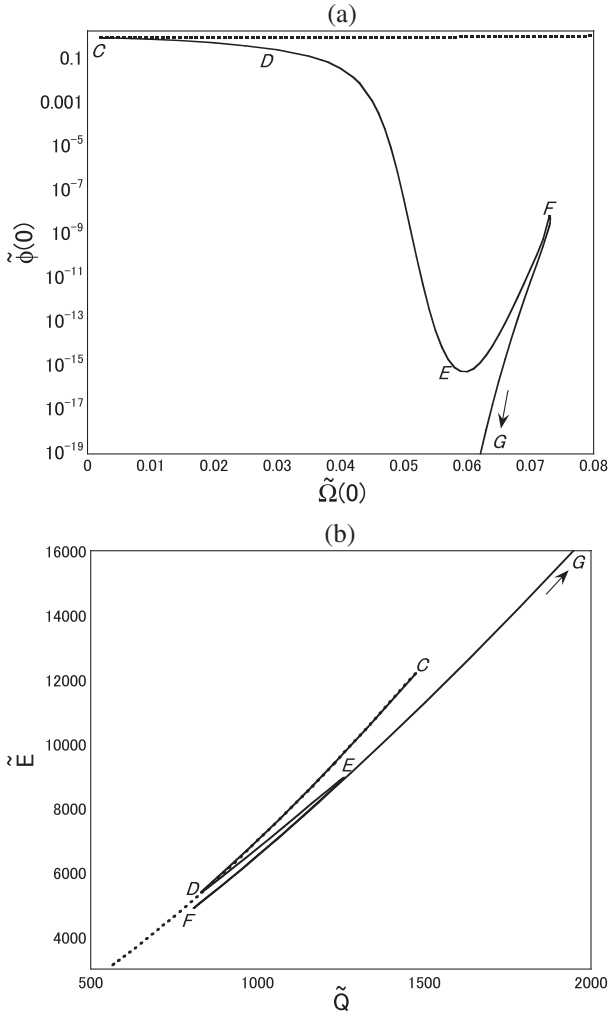

FIG. 13. (a) $\tilde{\Omega}(0)$-$\tilde{\phi}(0)$ and (b) $\tilde{Q}$-$\tilde{E}$ relations for $K = -1.07$ and $\tilde{Q} > 500$. The dotted lines extend from Fig. 12.

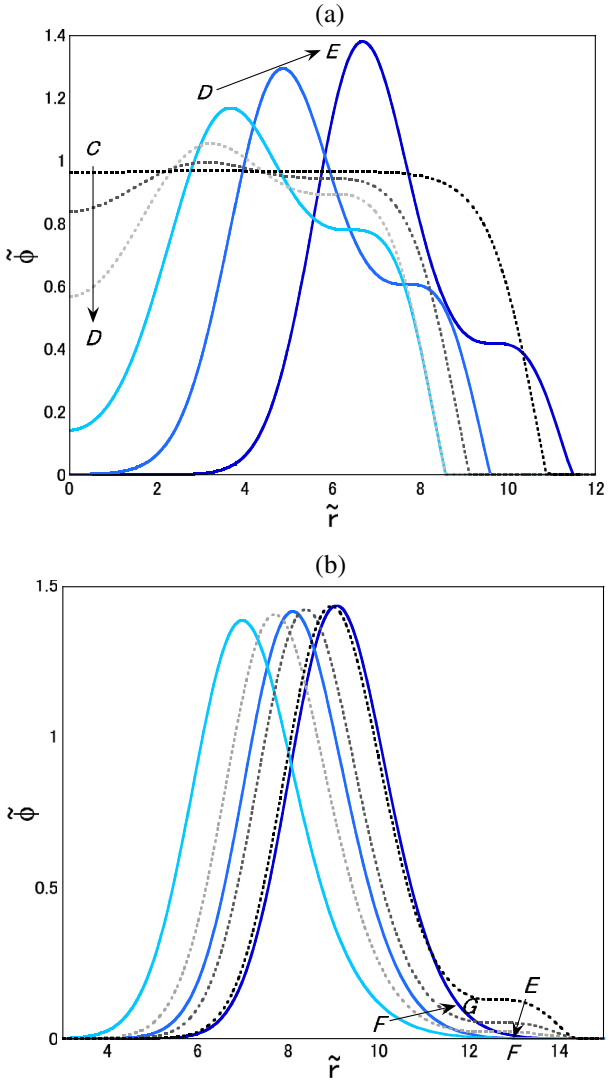

FIG. 14 (color online). Field distributions of $\tilde{\phi}$ with $K = -1.07$ for (a) solutions *C*-*D*-*E* and (b) solutions *E*-*F*-*G*.

VII. SUMMARY AND DISCUSSIONS

In many models of gauged Q-balls, which were studied in the literature, there are upper limits for charge $Q_{\max}$ and size of Q-balls due to the repulsive Coulomb force. The only known model that allows large Q without limitation is the V-shaped potential $V_{\rm V}$, which is singular at $\phi = 0$. Moreover, large Q solutions exist not as Q-balls but as Q-shells, which are obtained using boundary conditions (26). To make it clear whether property of unbounded Q is peculiar to the singular potential, we have derived general conditions for potentials that allow Q-balls with unbounded Q. We have found that large gauged Q-balls exist even for regular potentials.

One of the simple models is $V_{\log}$ in (39), which agrees with the gravity-mediated type of the Affleck–Dine mechanism. We have also investigated equilibrium solutions for this model systematically. As the electric charge Q increases, the field configuration of the scalar field becomes shell-like; because the charge is concentrated on the surface, the Coulomb force does not destroy the Q-ball configuration. These properties are analogous to Q-shells in $V_{\rm V}$, which was studied by Arodź and Lis [18], although we do not use boundary conditions (26). Thus, we can summarize this feature of gauged Q-balls as follows:

	Does $Q_{\max}$ exist?
V_4	Yes.
$V_{\rm V}$	Yes. ($Q_{\max}$ does not exist as a Q-shell.)
$V_{\log}$	No.

We have also found that for each K in $V_{\log}$ there are two sequences of solutions that can be seen in Figs. 8 to 11. These are summarized as follows:

(i) Unstable solutions written by red lines have small $\tilde{\Omega}(0)$, which has maximum $\tilde{\Omega}(0)_{\max}$. They have high-energy E comparing them with the stable solutions.

(ii) Stable solutions written by black lines have large $\tilde{\Omega}(0)$, which has minimum $\tilde{\Omega}(0)_{\rm min}$. They have low-energy E comparing them with the unstable solutions.

As $|K|$ increases, the two sequences approach. They are summarized in the table below. The value $\tilde{E}$ below is that for $\tilde{Q} = 50$, which is chosen as a reference:

	Unstable solutions	Stable solutions
$\lvert K\rvert = 0.4$	$\tilde{\Omega}(0)_{\rm max} \simeq 3.69 \times 10^{-5}$, $\tilde{E} \simeq 420$	$\tilde{\Omega}(0)_{\rm min} \simeq 1.3$, $\tilde{E} \simeq 98$
$\lvert K\rvert \nearrow$	$\tilde{\Omega}(0)_{\rm max} \nearrow$, $\tilde{E} \searrow$	$\tilde{\Omega}(0)_{\rm min} \searrow$, $\tilde{E} \nearrow$
$\lvert K\rvert = 1.06$	$\tilde{\Omega}(0)_{\rm max} \simeq 0.48$, $\tilde{E} \simeq 129.5$	$\tilde{\Omega}(0)_{\rm min} \simeq 0.70$, $\tilde{E} \simeq 129$

Eventually, at some point $K_{\rm crit.}$ in $-1.07 < K < -1.06$, the recombination of the two sequences takes place. This occurs at points A and B in Fig. 12. At first sight, this recombination looks strange. However, if we consider the existing domain in the three-dimensional parameter by regarding K as another parameter, it is described by a simply connected surface. The recombination of the two sequences is nothing but changing cross sections of the same surface.

ACKNOWLEDGMENTS

We would like to thank Kei-ichi Maeda for continuous encouragement. The numerical calculations were carried out on SX8 at YITP in Kyoto University.

[1] S. Coleman, Nucl. Phys. **B262**, 263 (1985).
[2] A. Kusenko, Phys. Lett. B **405**, 108 (1997); Nucl. Phys. B Proc. Suppl. **62A-C**, 248 (1998).
[3] I. Affleck and M. Dine, Nucl. Phys. **B249**, 361 (1985).
[4] K. Enqvist and J. McDonald, Phys. Lett. B **425**, 309 (1998); Nucl. Phys. **B538**, 321 (1999); S. Kasuya and M. Kawasaki, Phys. Rev. D **62**, 023512 (2000).
[5] A. Kusenko and M. Shaposhnikov, Phys. Lett. B **418**, 46 (1998); K. Enqvist, S. Kasuya, and A. Mazumdar, Phys. Rev. D **66**, 043505 (2002)K. Enqvist and A. Mazumdar, Phys. Rep. **380**, 99 (2003); I. M. Shoemaker and A. Kusenko, Phys. Rev. D **80**, 075021 (2009).
[6] A. Kusenko, M. Shaposhnikov, P. G. Tinyakov, and I. I. Tkachev, Phys. Lett. B **423**, 104 (1998).
[7] A. Kusenko, Phys. Lett. B **404**, 285 (1997); **406**, 26 (1997); T. Multamaki and I. Vilja, Nucl. Phys. **B574**, 130 (2000); M. Axenides, S. Komineas, L. Perivolaropoulos, and M. Floratos, Phys. Rev. D **61**, 085006 (2000); M. I. Tsumagari, E. J. Copeland, and P. M. Saffin, Phys. Rev. D **78**, 065021 (2008); E. Ya. Nugaev, and M. N. Smolyakov, J. High Energy Phys. 07 (2014) 009.
[8] F. Paccetti Correia and M. G. Schmidt, Eur. Phys. J. C **21**, 181 (2001).
[9] N. Sakai and M. Sasaki, Prog. Theor. Phys. **119**, 929 (2008).
[10] T. Tamaki and N. Sakai, Phys. Rev. D **81**, 124041 (2010); **83**, 044027 (2011); **83**, 084046 (2011); **84**, 044054 (2011).
[11] Y. Brihaye, B. Hartmann, and E. Radu, Phys. Lett. B **607**, 17 (2005); Y. Brihaye and B. Hartmann, Nonlinearity **21**, 1937 (2008); Phys. Rev. D **79**, 064013 (2009); Y. Brihaye, T. Caebergs, B. Hartmann, and M. Minkov, Phys. Rev. D **80**, 064014 (2009); B. Hartmann, B. Kleihaus, J. Kunz, and M. List, Phys. Rev. D **82**, 084022 (2010); B. Hartmann and J. Riedel, Phys. Rev. D **86**, 104008 (2012); B. Hartmann, B. Kleihaus, J. Kunz, and I. Schaffer, Phys. Lett. B **714**, 120 (2012); B. Hartmann and J. Riedel, Phys. Rev. D **87**, 044003 (2013); Y. Brihaye, B. Hartmann, and S. Tojiev, Classical Quantum Gravity **30**, 115009 (2013); B. Hartmann, J. Riedel, and R. Suciu, Phys. Lett. B **726**, 906 (2013); B. Hartmann, B. Kleihaus, J. Kunz, and I. Schaffer, Phys. Rev. D **88**, 124033 (2013).
[12] N. Sakai, H. Ishihara, and K. Nakao, Phys. Rev. D **84**, 105022 (2011).
[13] T. Tamaki and N. Sakai, Phys. Rev. D **86**, 105011 (2012).
[14] K. Lee, J. A. Stein-Schabes, R. Watkins, and L. W. Widrow, Phys. Rev. D **39**, 1665 (1989).
[15] K. N. Anagnostopoulos, M. Axenides, E. G. Floratos, and N. Tetradis, Phys. Rev. D **64**, 125006 (2001).
[16] Xin-zhou Li, Jian-gang Hao, and Dao-jun Liu, J. Phys. A **34**, 1459 (2001).
[17] M. Deshaies-Jacques and R. MacKenzie, Can. J. Phys. **85**, 693 (2007).
[18] H. Arodź and J. Lis, Phys. Rev. D **79**, 045002 (2009).
[19] I. E. Gulamov, E. Ya. Nugaev, and M. N. Smolyakov, Phys. Rev. D **89**, 085006 (2014).
[20] For a review of catastrophe theory, see, e.g., T. Poston and I. N. Stewart, *Catastrophe Theory and Its Application* (Pitman, New York, 1978).